Desalination and Water Treatment
www.deswater.com
doi: 10.5004/dwt.2019.24461

168 (2019) 77–87
November

Synthesis and characterization of activated carbon fibers derived from corn silk and its application in *p*-Cresol removal

Muhammad Ashraf Sabri[a], Taleb Hassan Ibrahim[a,*], Yehya Amin El Sayed[b]

[a]*Department of Chemical Engineering, American University of Sharjah, P.O. Box: 26666 Sharjah, UAE, Tel. +971507769239; email: italeb@aus.edu (T.H. Ibrahim)*
[b]*Department of Chemistry, Biology and Environmental Sciences, American University of Sharjah, P.O. Box: 26666 Sharjah, UAE*

Received 13 December 2018; Accepted 27 May 2019

ABSTRACT

This study reports the synthesis of activated carbon fibers (ACF) from corn silk via physical and chemical activation using CO_2 and KOH as activation agents, respectively. The influence of activation temperature, mode of activation, and an activation agent (KOH) to fiber (A/F) ratio on the texture, structure, and pore characteristics of ACF were investigated. ACF were characterized using scanning electron microscopy, Fourier transform infrared spectroscopy, thermogravimetric analysis, and nitrogen adsorption–desorption isotherm studies. The characterization results indicate that the corn silk was successfully converted into thermally stable microporous ACF while retaining their fibrous form. The optimum A/F ratio and activation temperature of chemically activated carbon fibers (CACF) were found to be 3 and 850°C providing a highly porous structure and a specific surface area of 1,363 m^2/g. The maximum surface area in case of physically activated carbon fibers (PACF) at optimum conditions was determined to be 934 m^2/g. The synthesized ACF adsorption experimentation was carried out with *p*-Cresol adsorption. The adsorption of *p*-Cresol on ACF followed Langmuir isotherm and the maximum adsorption capacity of CACF and PACF was determined to be 476 and 400 mg/g, respectively. The reaction kinetics of *p*-Cresol on ACF was found to follow pseudo-second-order kinetics model with reaction rates of 0.0055 g/mg min and 0.015 g/mg min for CACF and PACF, respectively. The removal efficiency of *p*-Cresol using CACF and PACF exceeded 97% and 75%, respectively, at optimum conditions. These results imply that corn fiber–based ACF can be used effectively as an adsorbent for the removal of *p*-Cresol from wastewater steams.

Keywords: Corn silk; BET surface area; Organic removal; Adsorption isotherms; Kinetic studies; Corn silk activated carbon

1. Introduction

The term "wastewater treatment" became quite common recently because of the enormous adverse effects of wastewater on the environment and living organisms. The wastewater generated is of several types depending on the community, the industry, and the system under consideration. Certain types of wastewater, such as produced wastewater or textile wastewater, are produced as a result of processes occurring in oil fields and textile industries. Voluminous amounts of wastewater are discharged into water bodies every day, this may cause a potential threat for the quality of the downstream water body and aquatic life survival [1–4]. Several useful techniques are being utilized for the effective treatment of industrial wastewater, but each of these techniques has inherent negative impacts in one way or the other [2–4]. Chemical treatment requires a lot of expensive and toxic chemicals that are potentially hazardous to life and the environment; then there is treatment via physical methods, which mostly ends up with

* Corresponding author.

excessive sludge that is still a major concern to deal with [4–7]. Adsorption is still considered to be the most effective method for the treatment of dyes, oil, and organic matters such as phenols in industrial wastewaters; however, their use is limited due to their lower capacity per gram and high costs [8,9]. This leads one to the conclusion that the introduction of novel technologies and adsorbents is necessary to enhance the removal efficiency, cost effectiveness, and environmental friendliness of the treatment processes. Several adsorbents are used to remove organic wastewater; such as granular activated carbon, activated carbon (AC), and carbon fibers (CF). However, activated carbon fibers (ACF) are more efficient in comparison with other nano-porous carbon materials [10–13]. This is due to their small diameters, high surface area, and excellent adsorption capacity.

Waste biomass utilization can be regarded as a sustainable alternative for ACF production from synthetic sources as well as for solid waste disposal. Several studies have been reported for the use of biowaste as adsorbents (biosorbents) for organics and heavy metal removal from wastewater streams [14–18]. Petrović et al. [19] reported the use of corn silk (CS) for the removal of lead from aqueous streams with a maximum adsorption capacity up to 90 mg/g. Similarly, mechanism of heavy metals (Cu^{2+} and Zn^{2+}) adsorption on CS have been reported showing good adsorption characteristics of CS [17]. In this study, ACF from naturally abundant and low-cost waste biomass (CS) were prepared and compared. The available biomass was carbonized, without the need of stabilization, at elevated temperatures under a nitrogen atmosphere. The carbonized fibers were activated using physical and chemical modes of activation. The physical activations were carried out using carbon dioxide and steam while the chemical activation was done using potassium hydroxide. The experimental parameters were optimized using flowrates, carbonization and activation, temperature and time, and carbon fiber/activation agent ratio. The structure and morphology of the developed ACF were studied using Fourier transform infrared spectroscopy (FT-IR), scanning electron microscopy (SEM), and energy dispersive X-ray spectroscopy (EDS). The thermal properties were investigated using thermogravimetric analysis (TGA). The pore size distribution, along with the structural parameters, was measured using nitrogen sorption isotherms. The results showed the development of ACF with a promising surface area and structure. The surface features indicate that the developed ACF can be employed in a variety of air and water applications. The efficiency of the prepared ACF as adsorbents for the removal of organics such as phenols, cresols and dyes from wastewater streams and produced water treatment were investigated. The adsorption isotherm, kinetics, and thermodynamics of the adsorption of these organic pollutants on ACFs were studied.

Preliminary studies indicated high removal efficiency of oil from produced water and phenols and dyes from wastewater streams. The adsorption study on the synthesized ACF from CS gave a higher removal efficiency of 97% of cresol from wastewater. The structure, morphology, thermal properties, pore size distribution (along with structural properties), surface area, adsorption parameters, yield, and the efficiency of ACF (prepared from waste biomass at different temperature and modes of activation) were compared. The ACF from chemical activation (CACF) exhibit higher surface area as compared with surface area of ACF from physical activation (PACF).

2. Materials and instrumentation

2.1. Materials

CS was obtained from Salalah, Oman. *p*-Cresol, KOH pellets, NaOH and HCl were purchased from Sigma-Aldrich (Milan, Italy), Emsure (Sigma-Aldrich, Darmstadt, Germany), and AppliChem Panreac (Darmstadt, Germany), respectively.

2.2. Instrumentation

CSs were carbonized and activated in a high temperature tube furnace (OTF-1200X, MTI Corporation, CA, USA). A pH meter (3320, JENWAY Ltd., Staffordshire, UK) was used for pH measurements. A temperature-controlled flask shaker (TH 15, Edmund Buhler, Bodelshausen, Germany) was utilized at 150 rpm for temperature control and shaking. *p*-Cresol was analyzed using UV–Vis spectrophotometer (DR-5000, HACH, USA) at a wavelength of 278.0 nm. FT-IR spectroscopy (Bomem MB-3000 equipped with ZnSe optics and a DTGS detector, Pectrum One FT-IR Spectrum, PerkinElmer, Australia) was used to study the functional groups on the sample's surface. SEM and EDS (TESCAN VEGA.3-LMU, USA) were used to observe the surface morphology and for percentage elemental analysis determination, respectively. A thermal analyzer (TA: PerkinElmer thermal analyzer CT06484-4794, USA) was used to obtain differential thermogravimetric (DTG) and themogravimetric (TG) curves. The pore characteristics and surface area were determined using Quantachrome (Quantachrome instruments, ASIQM0VJ010-4, Boynton Beach, FL, USA).

2.3. Preparation of activated carbon fibers

CS was washed thoroughly with water, and then rinsed with distilled water to remove dirt and impurities attached to the surface. The washed CS was air dried. Carbonization of the CS was carried out in a horizontal tube furnace under nitrogen gas flow of 135 mL/min at 850°C for 1 h with heating rate of 10°C/min. The carbonized CS (CF) was activated using physical and chemical activation routes in a horizontal tube furnace at different temperatures for 1 h. Physical activation was done using carbon dioxide at a flowrate of 250 mL/min while the chemical activation was carried out using potassium hydroxide under nitrogen flow (250 mL/min) at different temperatures (750°C–900°C) [20]. The carbonized fibers were heated at a heating rate of 10°C/min till the activation temperature. In case of chemical activation, the required amount of KOH was dissolved in water and then mixed with carbonized CS in pre-weighed quantity. This mixture was then put in the tube furnace immediately for pyrolysis [20]. The chemically activated carbon fibers (CACF) were neutralized using nitric acid. The ACF were dried in an oven at 110°C and stored in desiccators.

The samples were named according to the following routine, "mode of activation, ACF, activation temperature"

such as PACF800 refers to physically activated carbon fibers (PACF) at 800°C. In case of CACF, the ratio of KOH to fiber mass (impregnation ratio) for activation is indicated at the end, for example, CACF850-3 refers to ACF that were activated using KOH at 850°C with an impregnation ratio of 3.

2.4. Characterization

The ACF samples were initially placed in an oven at 110°C for one hour to ensure moisture removal before characterization. The characterization of CS, carbonized fibers (CF), and ACF were carried out in terms of their morphology, pore structure, pore characteristics, thermal stability, surface elemental composition, and the functional groups present. The functional groups present on the surface of these samples were studied using FT-IR (KBr method) within a scanning range of 400–4,000 cm^{-1}. The surface morphology was observed using SEM. Surface elemental composition of the samples was determined using EDS. For nitrogen adsorption isotherms, the samples were degassed at 120°C for 16 h under vacuum and then analyzed using Quantachrome (ASIQM0VJ010-4, USA). Brunauer–Emmett–Teller (BET) surface area, pore structure, and average pore size distribution were estimated using nitrogen adsorption at –195°C (Quantachrome, ASIQM0VJ010-4, USA) by applying the BET model. The thermal stability of the samples was studied through TGA, using a thermal analyzer (TA: PerkinElmer thermal analyzer CT06484-4794, USA) under a nitrogen atmosphere (nitrogen flow rate = 20 mL/min, heating rate = 10°C/min, range = 30°C–950°C, respectively).

2.5. Adsorption of organics (p-Cresol)

p-Cresol adsorption studies were carried out at batch bench scale to find the optimum adsorption parameters, kinetics, and adsorption capacity of the ACF prepared from corn silk. Stock *p*-Cresol solution of 500 mg/L was prepared by dissolving 0.5 g of *p*-Cresol in 1,000 mL of distilled water. The stock solution was diluted with distilled water to the desired concentration. The *p*-Cresol calibration curve was prepared by absorbance measurements of *p*-Cresol solutions with known concentrations at 278.0 nm using a UV–Vis spectrophotometer (DR-5000, HACH, USA). Batch bench-scale experiments, pre-weighed adsorbent amount was added to 50 mL of *p*-Cresol solution of known concentration and agitated at 150 rpm for 2 h. The *p*-Cresol concentration after adsorption was quantified spectrophotometrically at 278.0 nm.

The amount of *p*-Cresol adsorbed on the ACF was calculated using the following equation:

$$q_t = \frac{C_0 - C_t}{m_{\mathrm{ad}/v}} \tag{1}$$

where q_t and $m_{\mathrm{ad}/v}$ represent the mass of *p*-Cresol adsorbed per unit mass of ACF (mg/g) at a specific time and the mass of adsorbent (ACF) per unit volume used (g/L). C_0 and C_t are the *p*-Cresol concentrations of the sample before and after adsorption (mg/L), respectively.

Similar adsorption experiments were carried out at different adsorption parameters: ACF dosage (0.1–2 g/L), contact time (0–120 min), pH (highly acidic to highly basic), temperature (25°C–50°C), solution volume (50 mL) and initial *p*-Cresol concentration (0–500 mg/L) in order to determine the optimum experimental parameters, kinetics, and adsorption capacity of the physically and chemically modified ACFs.

3. Results and discussion

3.1. Characterization

3.1.1. Thermogravimetric analysis

Fig. 1 shows the TG and DTG curves of raw CS and ACF samples. The behaviors of raw CS and ACF at elevated temperatures differ significantly. Fig. 1 shows that the ACF are stable as compared with CS, owing to the decomposition of functional groups within the temperature range of 150°C–500°C. Three main degradation peaks are obvious in case of CS (Fig. 1a). The first peak at between 40°C and 150°C corresponds to dehydration and loss of volatile materials. The peaks at 300 and 346 represent the decomposition of hemi-cellulosic materials, while the peak at 477°C is mainly due to the decomposition of lignin materials [21]. These peaks are absent in case of ACF due to the fact that these groups were decomposed during the carbonization step. In the case of ACF, the only decomposition peak is related to the moisture loss around 100°C. This moisture loss is higher in case of ACF as compared with raw CS. This is related to the high specific surface area and the hydrophilic nature of the ACF surface [22]. The higher the hydrophilic nature, the higher the moisture loss due to the absorbed moisture in the porous structure of the ACF samples. Similar results were reported by Alkathiri et al. [20]. Polyacrylonitrile based ACF, prepared at 850°C, were reported to be thermally stable from 100°C to 800°C with a mass loss due to moisture content at 100°C [20].

3.1.2. Texture characterization and surface morphology (SEM)

Fig. 2 shows the morphology of the CF and ACF. It is evident from Fig. 2 that the overall structure of the fibers remained unchanged after activation. In case of ACF (B and C), the surface exhibits a rough and porous morphology with irregular slits and pores on the surface. These slits and pores contribute to the increased surface area and adsorption capacities of the prepared ACF.

3.1.3. Pore characteristics (PSD)

Specific surface area and pore characteristics of ACF were determined using adsorption–desorption isotherms and BET plots of nitrogen at 77 K. Fig. 3b shows the nitrogen adsorption isotherms of prepared ACF. The shapes of the isotherms dictate an intermediate between type I and type IV isotherms indicating a combination of micro and mesoporous structure [22,23]. It is evident from Fig. 3b that activation of the carbon fibers at 850°C, despite of the activation method, resulted in enhanced nitrogen uptake. It is worth noting that activation at 850°C resulted in larger pores which is evident in the wider hysteresis loops on

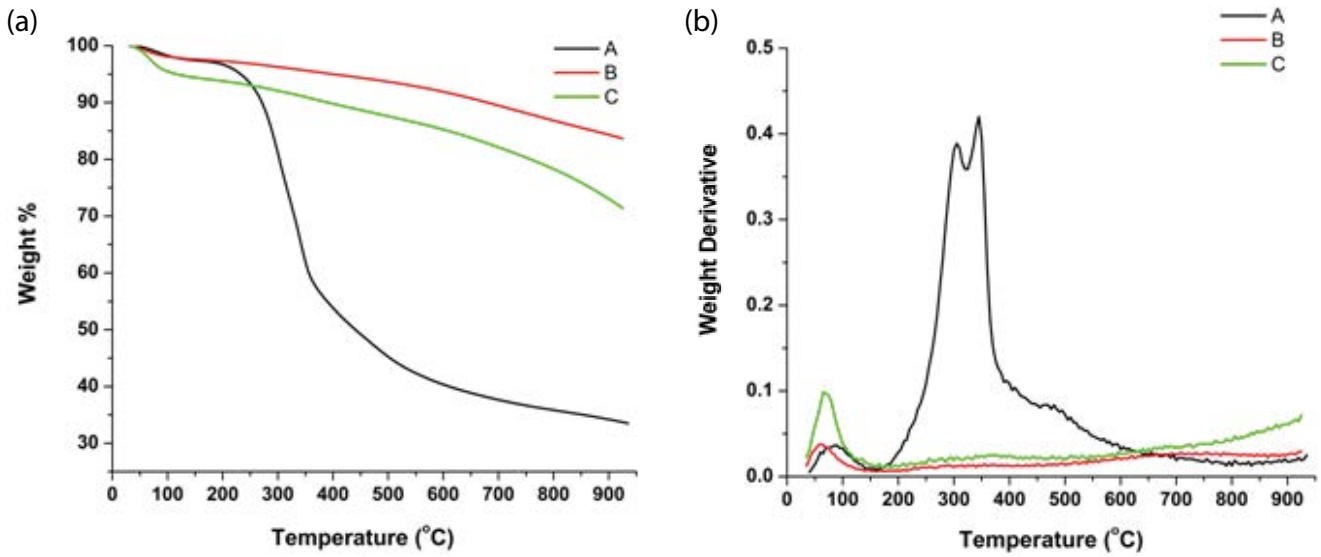

Fig. 1. (a) TG and (b) DTG curves of (A) raw CS, (B) CACF850-3, and (C) PACF850.

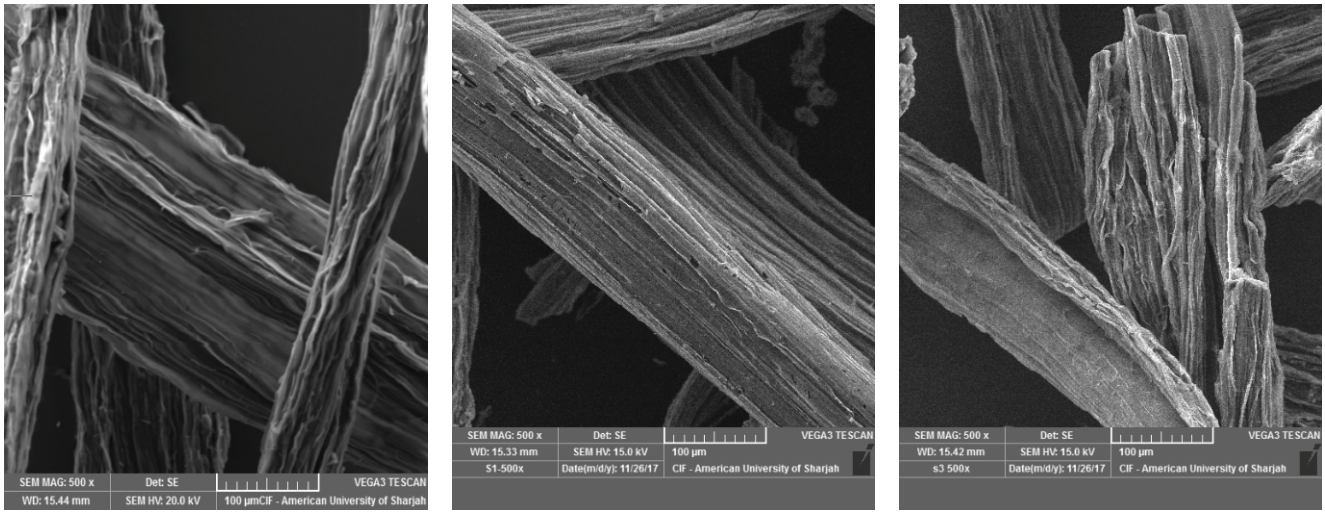

Fig. 2. SEM images of (a) CF, (b) CACF850-3, and (c) PACF850.

ACF prepared at 850°C compared with those activated at 800°C. Fig. 3a represents the pore size distribution (PSD) of the ACF. Table 1 presents the BET surface area, microporous volume, and the total volume of the ACF samples. Inspection of Fig. 3 and Table 1 dictates that (i) the specific surface area of the CACF is quite larger than PACF at same activation conditions. (ii) The specific surface area of CACF is increased from 1,058 to 1,159 m^2/g as the KOH to fiber ratio is increased from 1 to 3, which proves the formation of new pores due to increased KOH amount. (iii) The specific surface area of ACF increased by 200 m^2/g ca. as the temperature was increased from 800°C to 850°C. (iv) The ACF activated at 800°C are majorly microporous in structure, however the ACF activated at 850°C represents a combination of micropores and mesopores. (v) The volume of pores smaller than 20 Å are larger ACFs prepared at 850°C which appear to have larger volume of pores greater than 20 Å as well.

Mitravinda et al. [24] utilized a two-step conventional pyrolysis of CS for the production of activated carbon for supercapacitor applications. The CS was activated using impregnation ratio of 4:1 w/w at a temperature of 900°C for an activation time of 1 h with heating rate of 5°C min^{-1} in nitrogen atmosphere. The resulting activated carbon provided a surface area of 1,246 m^2/g with V_t of 0.7 cm^3/g [24]. The CACF prepared in this study were prepared at lower activation temperature (850°C) and with less use of chemical (3:1). However, the resulting porosity and surface area of the CACF850-3 is higher than that prepared by the above-mentioned literature works.

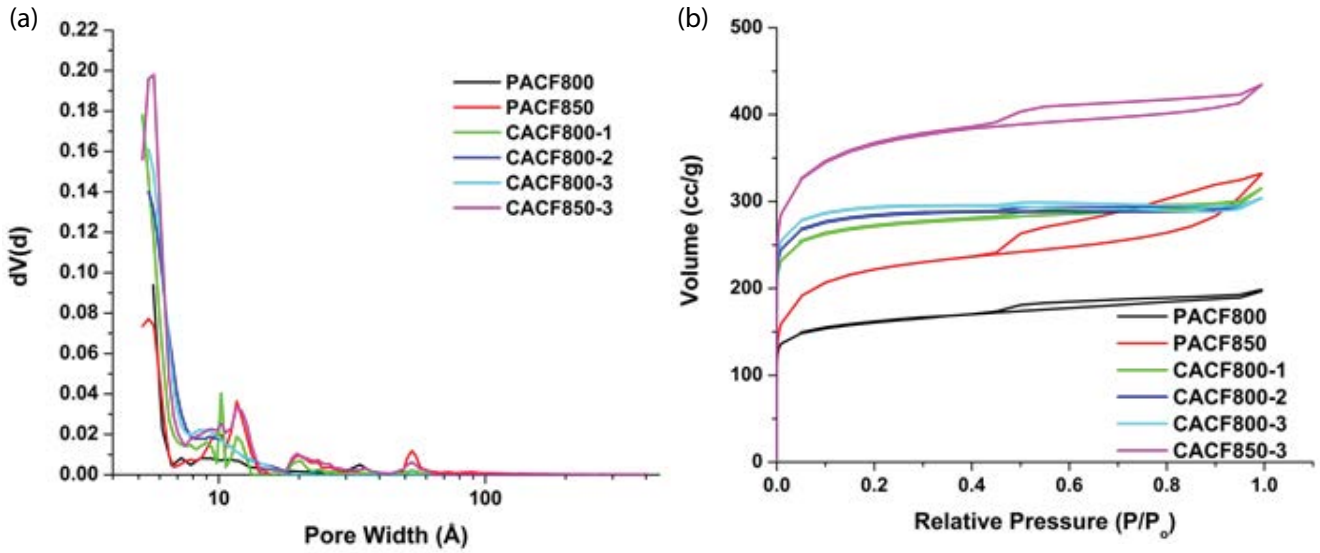

Fig. 3. (a) Pore size distribution and (b) Nitrogen adsorption–desorption isotherms at 77 K of ACF samples.

Table 1
Surface area, pore volumes, and activation conditions of different ACFs synthesized from CS

Sample	Surface area (m^2/g)	$V_{DFT<10Å}$ (cm^3/g)	$V_{DFT<20Å}$ (cm^3/g)	$V_{DFT\text{-}total}$ (cm^3/g)
CACF800-1	1,058	0.3484	0.4044	0.4695
CACF800-2	1,115	0.3556	0.4154	0.4176
CACF800-3	1,159	0.3716	0.4289	0.4314
CACF850-3	1,363	0.3752	0.4909	0.6420
PACF800	618	0.1909	0.2267	0.2806
PACF850	934	0.1668	0.2604	0.4952

3.1.4. Surface chemistry (FT-IR)

Fig. 4 represents the FT-IR spectra of raw CS, CF, and ACF samples synthesized at different activation parameters. The absorbance band observed between 3,000 and 3,700 cm^{-1}, present in all samples, is attributed to hydroxyl group (OH) [25]. The absorbance intensity of this peak is relatively reduced in ACF as compared with raw CS. This decrease in peak intensity can be attributed to the moisture release and vaporization due to carbonization and activation processes at elevated temperatures. In addition, three strong peaks observed in CS at 2,917; 1,634; and 1,058 are assigned to C–H (for methyl and methylene functional groups present in cellulosic and hemi-cellulosic material) [25], C=C stretching in aromatic rings and C–O–C groups, respectively [12]. As apparent from Fig. 4, C–O–C and C=C peaks were highly diminished in the case of ACF samples. The C–H peaks disappeared in ACF suggesting complete removal of methyl and methylene related C–H functional groups. The peaks at 1,422; 1,270; and 805 are identical to in-plane C–H bending, C–O, and epoxy groups, respectively [12,25,26]. These peaks are slightly present in carbonized samples, however they are completely removed in all ACF samples. A detailed study of Fig. 4 indicates the removal of major peaks and functional groups from raw CS as the carbonization followed by activation of CS at elevated temperatures (particularly at 850°C) is carried out. It is interesting to note that in comparison with CACF and PACF, the peaks are more diminished in the former than in the later, suggesting effective removal of functional groups on CS surface using alkali treatment. A detailed study of the Figs. 4D and I reveals that there is no difference in the FT-IR spectra of PACF850 before and after adsorption. This can be speculated due to ionic adsorption and weak electrostatic interactions between adsorbent and adsorbate [27].

3.2. Adsorption

The *p*-Cresol adsorption on ACFs has been studied and reported in the following sections. The effect of initial pH, adsorption dosage, initial concentration, and time were studied. The kinetics and isotherms of *p*-Cresol adsorption on ACFs have also been reported in the proceeding sections. In all cases, CACF850-3 and PACF850 were used in adsorption studies, respectively.

3.2.1. Effect of initial pH

The effect of the initial pH on CACF850-3 and PACF850 is demonstrated in Fig. 5. It is obvious that the removal efficiency in the case of CACF850-3 is independent of the initial pH. In the case of PACF850, the initial pH plays an

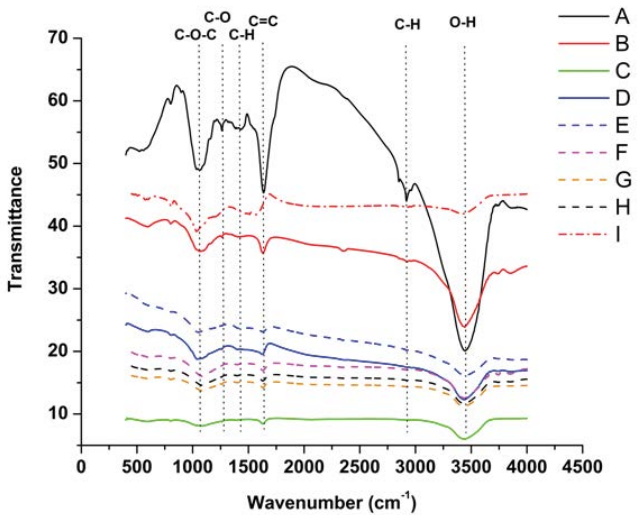

Fig. 4. FT-IR of CS (A), CF (B), CACF850-3 (C), PACF850 (D), PACF800 (E), CACF800-3 (F), CACF800-2 (G), CACF800-1 (H), and PACF850 after adsorption (I).

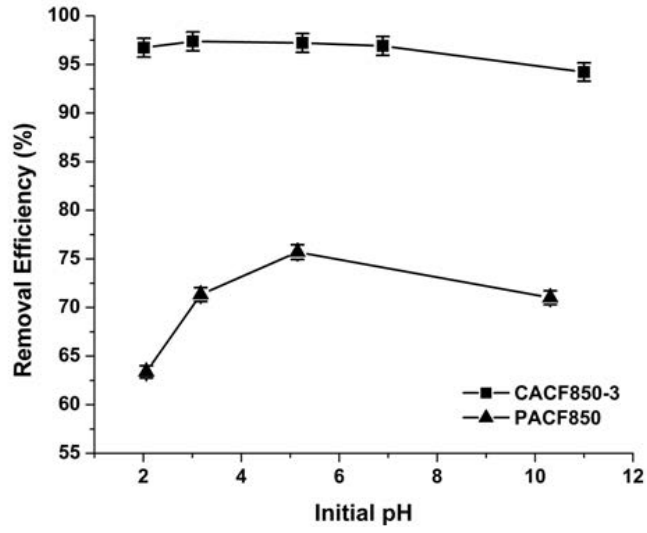

Fig. 5. Effect of initial pH on the removal efficiency of p-cresol using CACF850-3 and PACF850. Experimental conditions include: adsorbent dosage: 1 g/L, contact time: 2 h, temperature: 25°C, initial p-cresol concentration: 200 mg/L, solution volume: 50 mL, and stirring speed: 150 rpm.

important role in the removal efficiency of *p*-Cresol. The PACF850 has high removal efficiency for *p*-Cresol in slightly acidic and basic media while the removal efficiency decreases at highly alkaline or highly acidic media. This difference in the behavior of CACF850-3 and PACF850 can be explained in terms of their activation conditions. CACF850-3 were prepared at highly alkaline conditions and were neutralized with an acidic media, this might explain the reason for their independent nature with respect to initial pH conditions of the solution as the pores were conditioned with both acidic and basic media. Such treatment can lead to changes in the surface chemistry of the prepared ACF. Further details on the effects of ACF chemistry on the adsorption of organics from aqueous solutions has been provided by Li et al. [28]. In case of PACF850, the pores were not exposed to extreme pH conditions. CACF850-3, having a highly porous structure with high surface area as compared with the porous structure and surface area of PACF850, is able to remove above 95% of *p*-Cresol from aqueous solutions at all pH.

3.2.2. Effect of dosage

Fig. 6 presents the effect of adsorbent dosage on the removal efficiency of *p*-Cresol using CACF850-3 and PACF850. As obvious from the figure, the removal efficiency of both ACF increases rapidly with an initial increase in the adsorbent dosage. A further increase in the adsorbent dosage above 1 g/L shows a very slight change in the removal efficiency of *p*-Cresol. It is interesting to note that at similar dosage conditions, the CACF850-3 was able to remove more *p*-Cresol as compared with the removal efficiency of *p*-Cresol using PACF850. This can be attributed to the high surface area of CACF850-3 providing more adsorption sites as compared with PACF850.

3.2.3. Effect of contact time and kinetic studies

The study of the effect of contact time on the removal efficiency of *p*-Cresol is necessary to determine the adsorption kinetics, equilibrium time, and economic feasibility of the process. Fig. 7 illustrates the change in the removal efficiency of *p*-Cresol on ACFs as time changes from 0 to 120 min. The optimum time in case of CACF850-3 and PACF850 is 60 and 30 min, respectively. The CACF850-3 has a highly porous network and relatively high number of pores, the equilibrium time is higher as the intraparticle diffusion in the pores of ACF is slightly slower. This could further be explained in

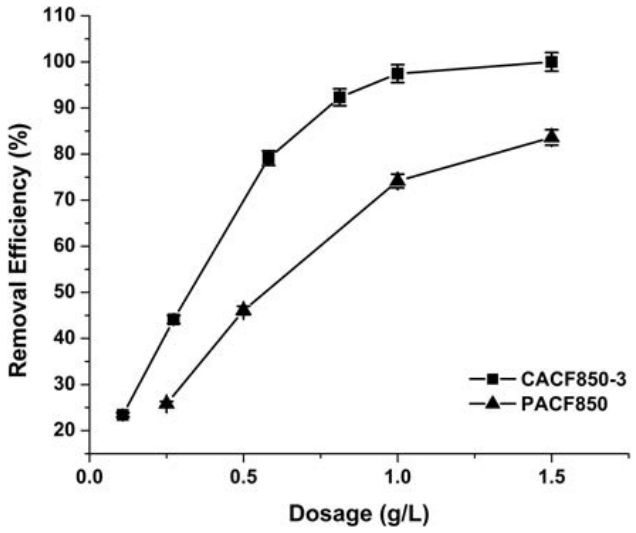

Fig. 6. Effect of adsorbent dosage on the removal efficiency of p-cresol using CACF850-3 and PACF850. Experimental conditions include: initial pH: 5.25, contact time: 2 h, temperature: 25°C, initial p-cresol concentration: 200 mg/L, solution volume: 50 mL, and stirring speed: 150 rpm.

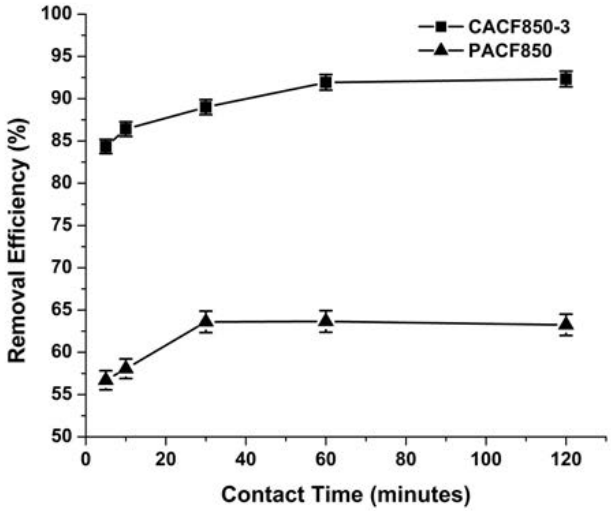

Fig. 7. Effect of contact time on the removal efficiency of p-cresol using CACF850-3 and PACF850. Experimental conditions include: initial pH: 5.25, adsorbent dosage: 0.6 g/L, temperature: 25°C, initial p-cresol concentration: 200 mg/L, solution volume: 50 mL, and stirring speed: 150 rpm.

terms of diffusion of *p*-Cresol onto ACF through various diffusion films and processes.

Adsorption kinetics is important in determining the equilibrium time, reaction path followed, and the adsorption mechanism of adsorbent uptake by the specific adsorbent [29,30]. Lagergren model (pseudo-first-order-kinetics) and pseudo-second-order-kinetics models are the most widely used kinetic models for adsorption studies [31,32]. The linearized form of these two models is given by Eqs. (2) and (3), respectively, as follows:

$$\ln\left(q_e - q_t\right) = -k_1 t + \ln q_e \tag{2}$$

$$\frac{t}{q_t} = \frac{t}{q_e} + \frac{1}{K_{II} q_e^2} \tag{3}$$

where t, q_t, and q_e represent time (min), adsorption capacity at specific time (mg/g), and equilibrium adsorbate uptake by the adsorbent or equilibrium adsorption capacity (mg/g). k_I and k_{II} are the rate constants for pseudo-first-order (1/min) and pseudo-second-order r (g/mg min), respectively. Fig. 8 represents the experimental data plotted according to the first and second order pseudo-kinetics-model. The high R^2 value for pseudo-second-order kinetics model, 0.99 for both ACFs, reflects excellent demonstration of the adsorption data by pseudo-second-order kinetics model. This pseudo-second-order kinetics model indicates the intraparticle diffusion of *p*-Cresol on the ACF. The corresponding kinetic parameters, as determined from the figures, are presented in Table 2.

3.2.4. Effect of initial concentration and isotherms

Figs. 9a and b illustrate the effect of initial *p*-Cresol concentration on the removal and adsorption efficiency of *p*-Cresol using ACF. It is obvious that both adsorbents followed similar trends. The removal efficiencies of both adsorbents declined appreciably as the initial *p*-Cresol concentration was increased. This can be explained on the basis of the finite number of active sites present. These sites get saturated at higher concentrations, thus decreasing the available number of active sites for remaining *p*-Cresol molecules to adsorb.

This experimental data were also fitted to determine the applicability of the two most widely used equilibrium isotherm models, the Langmuir and Freundlich isotherm models [27,33]. The linearized forms of these two models are provided in Eqs. (4) and (5), respectively:

$$\frac{C_e}{q_e} = \frac{1}{K_L q_m} + \frac{C_e}{q_m} \tag{4}$$

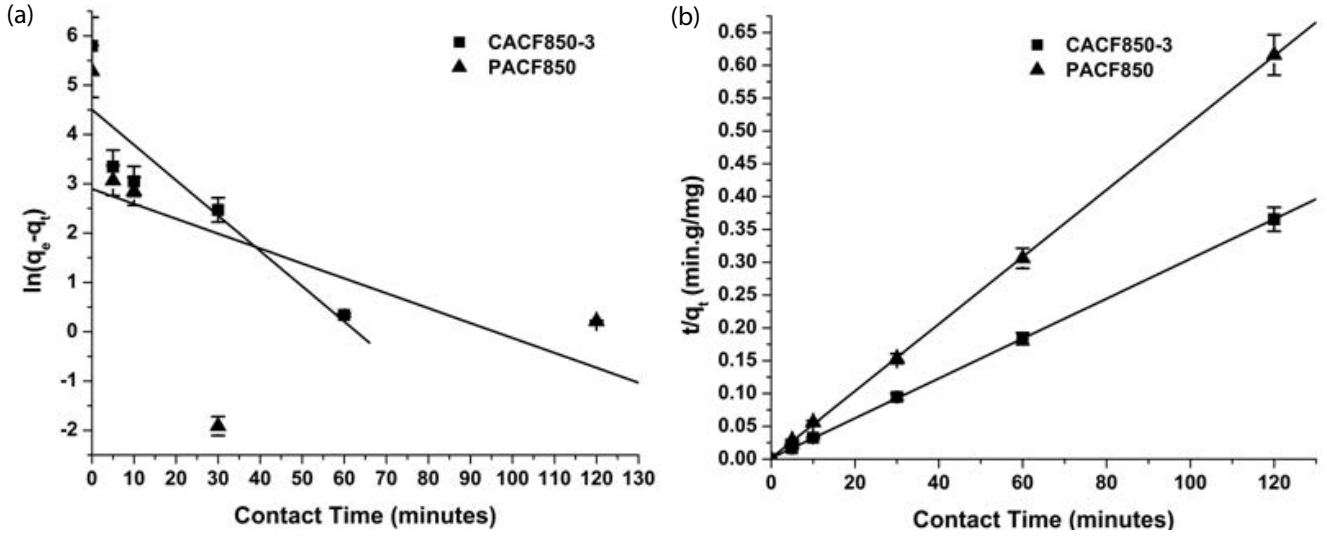

Fig. 8. Kinetic models (a) pseudo-first-order and (b) pseudo-second-order for p-cresol removal from aqueous solutions using ACF. Experimental conditions: adsorbent dosage: 0.6 g/L, initial p-cresol concentration: 200 mg/L, stirring speed: 150 rpm, solution volume: 50 mL, temperature: 25°C, pH: 5.25.

Table 2
Adsorption parameters of pseudo-first-order and pseudo-second-order kinetic models for p-cresol removal from aqueous solution using ACFs

ACF	Experimental q_e (mg/g)	Pseudo-first-order kinetic model			Pseudo-second-order kinetic model		
		k_1 (1/min)	q_e (mg/g)	R^2	k_{II} (g/mg min)	q_e (mg/g)	R^2
CACF850-3	328.4	0.072	90.29	0.81	0.0055	330.0	0.99
PACF850	194.9	0.032	16.45	0.32	0.015	195.7	0.99

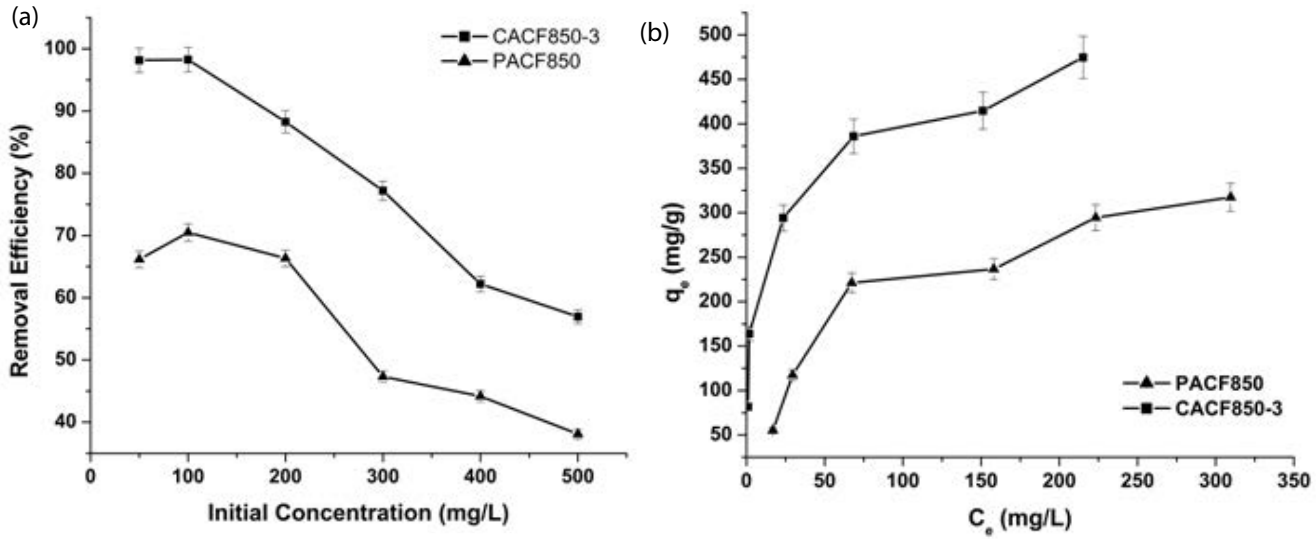

Fig. 9. Effect of initial concentration on the removal efficiency of p-cresol using CACF850-3 and PACF850. Experimental conditions include: initial pH: 5.25, adsorbent dosage: 0.6 g/L, temperature: 25°C, contact time: 2 h, solution volume: 50 mL, and stirring speed: 150 rpm.

$$\ln q_e = \ln k_f + n \ln C_e \quad (5)$$

where q_e, C_e, q_m, k_f, K_L, and n represent adsorbate mass adsorbed at equilibrium per gram of adsorbent (mg/g), equilibrium adsorbate concentration (mg/L), maximum adsorption capacity (mg/g), Freundlich capacity parameter ($mg^{(1-1/n)}L^{1/n}/g$), adsorption constants for Langmuir related to energy of adsorption, and adsorption constant for Freundlich related to adsorption intensity, respectively.

Fig. 10 shows the Langmuir and Freundlich isotherms and the corresponding experimental adsorption data of *p*-Cresol on ACFs. The relatively higher R^2 values in the case of Langmuir isotherms compared with that of Freundlich, indicates that the adsorption of *p*-Cresol is best described by Langmuir isotherms. This suggests the formation of the monomolecular layer of *p*-Cresol on the surface of the ACFs. The adsorption isotherm parameters for these adsorbents have been summarized in Table 3. The maximum adsorption capacity of the CACF850-3 is 476 mg/g larger as compared with the 400 mg/g of the PACF850. This can be explained in terms of the higher surface area of the CACF850-3 as compared with that of the PACF850 that was discussed earlier. The preparation and handling of PACP is easier and cheaper as it does not require the use of corrosive chemicals such as KOH (for activation) followed by neutralization by an acid. Consequently, the adsorption capacity of PACF is only a bit less in comparison with that of CACF. However, the ease in preparation and handling of PACF850 at the expense of the small decrease in the maximum adsorption capacity of PACF850 in comparison with CACF850-3 is acceptable.

Several studies have been reported for the removal of organics such as phenol and *p*-Cresol from aqueous solutions using different adsorbents. The maximum adsorption capacities of *p*-Cresol for these different bio-based adsorbents have been reported in Table 4.

These results indicate that CS based ACF having high adsorption capacities (>400 mg/g) can be used as a potential adsorbent for *p*-Cresol from aqueous solution. Furthermore, the CS is inexpensive, easily available and the ACF synthesis process from CS is quite straightforward.

3.2.5 Adsorption mechanism

Adsorption is known to involve three major steps namely film diffusion, particle diffusion and adsorption. Adsorption is typically a fast step thus particle diffusion or film diffusion can be the limiting step [37]. The liquid film model (Eqs. (6) and (7)) and intraparticle diffusion models, Eq. (8) can be expressed as [37,38]:

$$\ln\left[1 - F\right] = -K_{fd}t \quad (6)$$

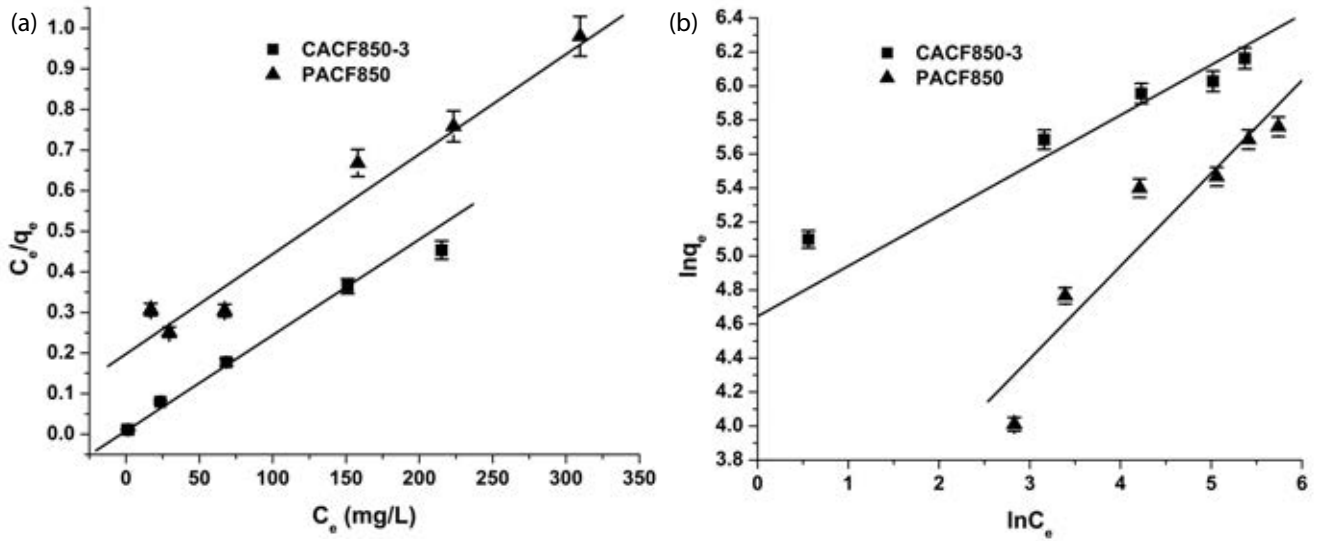

Fig. 10. Isotherm models (a) Langmuir, (b) Freundlich for the adsorption of p-cresol using CACF850-3 and PACF850. Experimental conditions include: initial pH: 5.25, adsorbent dosage: 0.6 g/L, temperature: 25°C, contact time: 2 h, solution volume: 50 mL, and stirring speed: 150 rpm.

Table 3
Adsorption parameters of two different isotherm models for p-cresol removal from aqueous solutions using PACF850 and CACF850-3

Adsorption isotherm model	Parameters		
		CACF850-3	PACF850
Langmuir isotherm	K_L (L/mg)	0.0129	0.0121
	q_m (mg/g)	476.2	400.0
	R^2	0.991	0.970
Freundlich isotherm	k_f (mg$^{(1-1/n)}$L$^{1/n}$/g)	109.2	38.85
	n	3.525	1.999
	R^2	0.933	0.907

$$F = \frac{q_t}{q_e} \tag{7}$$

$$q_t = K_{id} t^{1/2} + C \tag{8}$$

where K_{fd} and K_{id} represent liquid film diffusion constant and intraparticle diffusion rate constant, respectively.

A review of Figs. 11a and b shows linear trend for liquid film and intraparticle diffusion while the graphs does pass through origins. This indicates that other mechanisms, except liquid film and intraparticle diffusion, contribute to the rate limiting step [39]. The high value of the intercept (C) indicates high contribution of surface adsorption on the rate limiting step in this process [37,38].

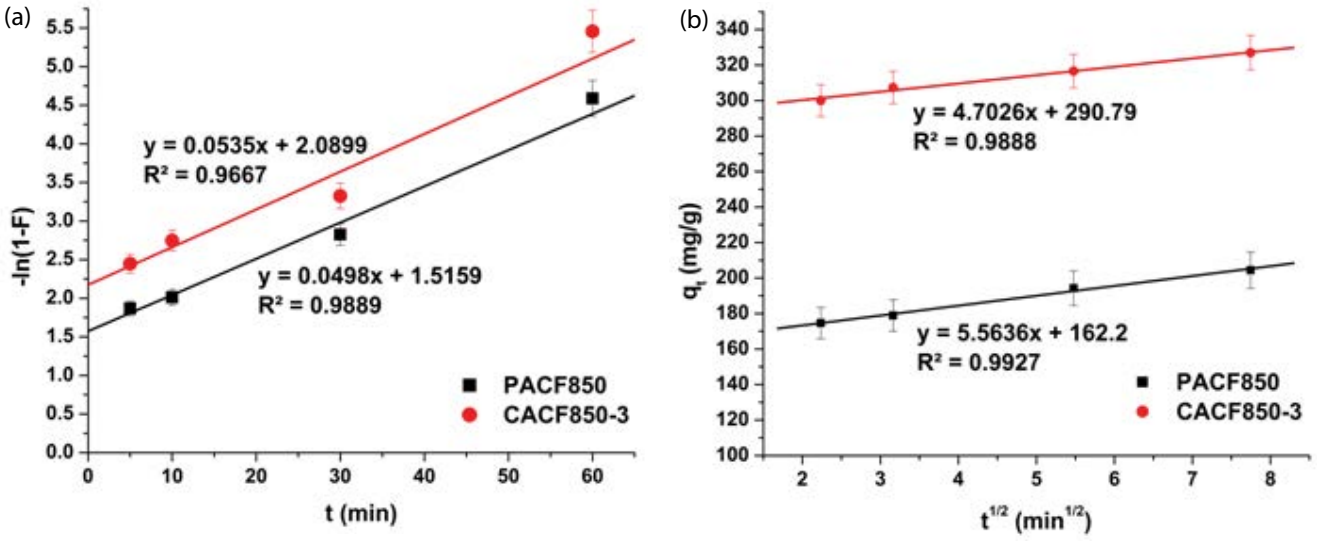

Fig. 11. Adsorption studies for adsorption of p-cresol on ACF from CS. (a) liquid film model and (b) intraparticle diffusion model.

Table 4
Maximum adsorption capacities of biosorbents for phenol and p-cresol removal

Absorbent	Adsorbate	Maximum adsorption capacity (mg/g)	Experimental conditions (adsorption)	Ref.
Pine wood AC	p-Cresol	6.97	Dosage: 10 g/L, temperature: 25°C, pH: unadjusted	[14]
Tobacco residue	Phenol	17.83	Dosage: 2 g/L, temperature: 20°C, pH: 7, contact time: 60 min	[15]
Coconut shell AC	p-cresol	32.77	Dosage: 10 g/L, temperature: 30°C, pH: 4, contact time: 24 h	[16]
Avocado seeds AC	p-Cresol	87.79	Dosage: 3 g/L, temperature: 25°C, contact time: 7 d	[34]
Luffa cylindrica fibers	Phenol	10.37	Dosage: 3 g/L, temperature: 20°C, pH: 7, contact time: 120 min	[35]
Coconut shell modified AC	Phenol	144.93	Dosage: 10 g/L, temperature: 25°C,	[36]
CACF850-3	p-Cresol	476.20	Dosage: 0.6 g/L, temperature: 25°C, pH: 5.25, contact time: 2 h	This work
PACF850	p-Cresol	400.0	Dosage: 0.6 g/L, temperature: 25°C, pH: 5.25, contact time: 2 h	This work

4. Conclusion

Carbon fibers, activated through physical and chemical modes, were synthesized from corn silk at different activation temperatures. The synthesized ACF were characterized using TGA, FT-IR, SEM, and nitrogen adsorption–desorption; this confirmed their thermal stability, functional groups present, morphology, and porosity. The BET surface area of these synthesized ACF ranged between 618 and 1,363 m^2/g. The CACF showed higher surface area (1,363 m^2/g) as compared with the surface area (934 m^2/g) of PACF at an activation temperature of 850°C. The adsorption of *p*-Cresol onto the ACFs followed Langmuir isotherms with maximum adsorption capacities of PACF and CACF determined to be 400 and 476 mg/g, respectively. *p*-Cresol adsorption on both adsorbents was confirmed to follow pseudo-second-order kinetics model with rate constants for PACF and CACF determined to be 0.015 and 0.0055 g/mg min, respectively. Adsorption experimentation confirmed that CACF is more efficient for *p*-Cresol removal from aqueous solutions as compared with PACF. At similar experimental conditions of adsorbent dosage (0.6 g/L) and contact time (30 min), CACF was able to remove 97% of *p*-Cresol from aqueous solutions as compared with 76% *p*-Cresol removal efficiency using PACF. These results prove that the synthesis of ACFs from corn silk is highly effective due to its relatively shorter activation time, well-developed porous structure, and high adsorption capacity. These characteristics of synthesized ACFs highlight its potential in air and wastewater treatment applications.

References

[1] Z. Khatib, P. Verbeek, Water to Value - Produced Water Management for Sustainable Field Development of Mature and Green Fields, SPE International Conference on Health, Safety and Environment in Oil and Gas Exploration and Production, Kuala Lumpur, Malaysia, March 20–22, 2002, pp. 1–3.
[2] A. Fakhru'l-Razi, A. Pendashteh, L.C. Abdullah, D.R.A. Biak, S.S. Madaeni, Z.Z. Abidin, Review of technologies for oil and gas produced water treatment, J. Hazard. Mater., 170 (2009) 530–551.
[3] C.F.M. Drumond, O.G.A. Rodrigues, F.E.R.l. Anastácio, C.J. Carvalho, Z.M. Valnice Boldrin, O. Danielle de Palma, In: M. Gunay, Eco-friendly textile dyeing and finishing, Intech Open, 2013, pp. 151–176.
[4] S.J. Kulkarni, J.P. Kaware, Review on research for removal of phenol from wastewater, Int. J. Sci. Res. Publ, 3 (2013) 1–5.
[5] F. Arena, C. Italiano, A. Raneri, C. Saja, Mechanistic and kinetic insights into the wet air oxidation of phenol with oxygen (CWAO) by homogeneous and heterogeneous transition-metal catalysts, Appl. Catal., B, 99 (2010) 321–328.
[6] A. Hussain, S.K. Dubey, V. Kumar, Kinetic study for aerobic treatment of phenolic wastewater, Water Resour. Ind., 11 (2015) 81–90.
[7] P.D. Vaidya, V.V. Mahajani, Insight into heterogeneous catalytic wet oxidation of phenol over a Ru/TiO2 catalyst, Chem. Eng. J., 87 (2002) 403–416.
[8] S. Babel, T.A. Kurniawan, Low-cost adsorbents for heavy metals uptake from contaminated water: a review, J. Hazard. Mater., 97 (2003) 219–243.
[9] F. Akhlaghian, M. Ghadermazi, B. Chenarani, Removal of phenolic compounds by adsorption on nano structured aluminosilicates, J. Environ. Chem. Eng., 2 (2014) 543–549.
[10] L. Giraldo, Y. Ladino, J.C.M. Pirajánc, M.P. Rodríguez, Synthesis and characterization of activated carbon fibers from Kevlar, Eclética Quím., 32 (2007) 55–62.
[11] S. Rafiei, B. Noroozi, A. Haghi, In: A.K. Haghi, S. Thomas, A. Pourhashemi, A. Hamrang, E. Klodzinska, Nanomaterials and Nanotechnology for Composites, CRC Press, 2015, pp. 359–418.
[12] C.H. Ooi, W.K. Cheah, Y.L. Sim, S.Y. Pung, F.Y. Yeoh, Conversion and characterization of activated carbon fiber derived from palm empty fruit bunch waste and its kinetic study on urea adsorption, J. Environ. Manage., 197 (2017) 199–205.
[13] M.A. Khan, B.H. Hameed, J. Lawler, M. Kumar, B.H. Jeon, Developments in activated functionalized carbons and their applications in decontamination: a review, Desal. Wat. Treat., 54 (2015) 422–449.

[14] L. Das, P. Kolar, J.J. Classen, J.A. Osborne, Adsorbents from pine wood via K_2CO_3-assisted low temperature carbonization for adsorption of *p*-Cresol, Ind. Crops Prod., 45 (2013) 215–222.
[15] M. Kilic, E. Apaydin-Varol, A.E. Pütün, Adsorptive removal of phenol from aqueous solutions on activated carbon prepared from tobacco residues: equilibrium, kinetics and thermodynamics, J. Hazard. Mater., 189 (2011) 397–403.
[16] Y. Zhu, P. Kolar, Adsorptive removal of *p*-Cresol using coconut shell-activated char, J. Environ. Chem. Eng., 2 (2014) 2050–2058.
[17] M. Petrović, T. Šoštarić, M. Stojanović, J. Petrović, M. Mihajlović, A. Ćosović, S. Stanković, Mechanism of adsorption of Cu^{2+} and Zn^{2+} on the corn silk (Zea mays L.), Ecol. Eng., 99 (2017) 83–90.
[18] V.A. Feisther, J.S. Filho, F.V. Hackbarth, D.A. Mayer, A.A.U. de Souza, S.M.A.G.U. de Souza, Raw leaves and leaf residues from the extraction of essential oils as biosorbents for metal removal, J. Environ. Chem. Eng., 7 (2019) 103047.
[19] M. Petrović, T. Šoštarić, M. Stojanović, J. Milojković, M. Mihajlović, M. Stanojević, S. Stanković, Removal of Pb^{2+} ions by raw corn silk (Zea mays L.) as a novel biosorbent, J. Taiwan Inst. Chem. Eng., 58 (2016) 407–416.
[20] D.S.S. Alkathiri, T.H. Ibrahim, Y.A. El Sayed, Development of activated carbon fibers for organic removals, MSChE, Department of Chemical Engineering, American University of Sharjah, Sharjah, UAE, 2017.
[21] M.G.L. Ramírez, G.I.B.de Muniz, K.G. Satyanarayana, V. Tanobe, S. Iwakiri, Preparation and characterization of biodegradable composites based on Brazilian cassava starch, corn starch and green coconut fibers, Matéria (Rio de Janeiro), 15 (2010) 330–337.
[22] A.F. Hassan, H. Elhadidy, Production of activated carbons from waste carpets and its application in methylene blue adsorption: kinetic and thermodynamic studies, J. Environ. Chem. Eng., 5 (2017) 955–963.
[23] X. Duan, C. Srinivasakannan, X. Wang, F. Wang, X. Liu, Synthesis of activated carbon fibers from cotton by microwave induced H_3PO_4 activation, J. Taiwan Inst. Chem. Eng., 70 (2017) 374–381.
[24] T. Mitravinda, K. Nanaji, S. Anandan, A. Jyothirmayi, V.S.K. Chakravadhanula, C.S. Sharma, T.N. Rao, Facile synthesis of corn silk derived nanoporous carbon for an improved supercapacitor performance, J. Electrochem. Soc., 165 (2018) A3369-A3379.
[25] H. Luo, G. Xiong, C. Ma, P. Chang, F. Yao, Y. Zhu, C. Zhang, Y. Wan, Mechanical and thermo-mechanical behaviors of sizing-treated corn fiber/polylactide composites, Polym. Test., 39 (2014) 45–52.
[26] R. Asadpour, N. Sapari, M.H. Isa, S. Kakooei, K.U. Orji, S. Daneshfozoun, Esterification of corn silk fiber to improve oil absorbency, Adv. Mater. Res., 1133 (2016) 552–556.
[27] J. Shim, M. Kumar, R. Goswami, P. Mazumder, B.-T. Oh, P.J. Shea, Removal of *p*-Cresol and tylosin from water using a novel composite of alginate, recycled MnO_2 and activated carbon, J. Hazard. Mater., 364 (2019) 419–428.
[28] L. Li, P.A. Quinlivan, D.R.U. Knappe, Effects of activated carbon surface chemistry and pore structure on the adsorption of organic contaminants from aqueous solution, Carbon, 40 (2002) 2085–2100.
[29] B. Saha, C. Orvig, Biosorbents for hexavalent chromium elimination from industrial and municipal effluents, Coord. Chem. Rev., 254 (2010) 2959–2972.
[30] A.S. Gulistan, Oil Removal from Produced Water Using Natural Materials, Master of Science in Chemical Engineering, Department of Chemical Engineering, American University of Sharjah, Sharjah UAE, 2014.
[31] S. Lagergren, Zur theorie der sogenannten adsorption geloster stoffe, K. Sven. Vetensk. Handl., 24 (1898) 1–39.
[32] Y.S. Ho, G. McKay, Sorption of dye from aqueous solution by peat, Chem. Eng. J., 70 (1998) 115–124.
[33] P.K. Gessner, M.M. Hasan, Freundlich and Langmuir isotherms as models for the adsorption of toxicants on activated charcoal, J. Pharm. Sci., 76 (1987) 319–327.
[34] Y. Zhu, P. Kolar, S.B. Shah, J.J. Cheng, P.K. Lim, Simultaneous mitigation of *p*-Cresol and ammonium using activated carbon from avocado seed, Environ. Technol. Innovation, 9 (2018) 63–73.
[35] O. Abdelwahab, N.K. Amin, Adsorption of phenol from aqueous solutions by Luffa cylindrica fibers: Kinetics, isotherm and thermodynamic studies, Egypt. J. Aquat. Res., 39 (2013) 215–223.
[36] D. Zhang, P. Huo, W. Liu, Behavior of phenol adsorption on thermal modified activated carbon, Chin. J. Chem. Eng., 24 (2016) 446–452.
[37] I.A.W. Tan, B.H. Hameed, Adsorption isotherms, kinetics, thermodynamics and desorption studies of basic dye on activated carbon derived from oil palm empty fruit bunch, J. Appl. Sci., 10 (2010) 2565–2571.
[38] T.J. Tarawou, E. Young, Intraparticle and liquid film diffusion studies on the adsorption of Cu^{2+} and Pb^{2+} ions from aqueous solution using powdered cocoa pod (Theobroma cacao), Int. Res. J. Eng. Technol., 2 (2015) 236–243
[39] M.M. Suliman, T.H. Ibrahim, F. Jumean, M.I. Khamis, M.A. Sabri, Removal of lead ions from wastewater using multi walled carbon nanotubes modified with sodium lauryl sulfate, Desal. Wat. Treat., 100 (2017) 55–66.